fluids

MDPI

Article

Thermal Performance Evaluation of Plate-Type Heat Exchanger with Alumina–Titania Hybrid Suspensions

Atul Bhattad [1], Boggarapu Nageswara Rao [1], Vinay Atgur [1,*], Ibham Veza [2], Mohd Faiz Muaz Ahmad Zamri [3] and Islam Md Rizwanul Fattah [4,*]

[1] Department of Mechanical Engineering, Koneru Lakshmaiah Education Foundation, Green Fields, Vaddeswaram, Guntur 522502, India
[2] Department of Mechanical Engineering, Universiti Teknologi PETRONAS, Bandar Seri Iskandar 32610, Perak Darul Ridzuan, Malaysia
[3] Institute of Sustainable Energy (ISE), Universiti Tenaga Nasional, Jalan Ikram-Uniten, Kajang 43000, Selangor, Malaysia
[4] Centre for Technology in Water and Wastewater (CTWW), School of Civil and Environmental Engineering, Faculty of Engineering and IT, University of Technology Sydney, Ultimo, NSW 2007, Australia
* Correspondence: atgurvinay@gmail.com (V.A.); islammdrizwanul.fattah@uts.edu.au (I.M.R.F.)

Abstract: This paper aims to develop models for the thermal conductivity and viscosity of hybrid nanofluids of aluminium oxide and titanium dioxide (Al_2O_3-TiO_2). The study investigates the impact of fluid temperature (283 K–298 K) on the performance of a plate heat exchanger using Al_2O_3-TiO_2 hybrid nanofluids with different particle volume ratios (0:5, 1:4, 2:3, 3:2, 4:1, and 5:0) prepared with a 0.1% concentration in deionised water. Experimental evaluations were conducted to assess the heat transfer rate, Nusselt number, heat transfer coefficient, Prandtl number, pressure drop, and performance index. Due to the lower thermal conductivity of TiO_2 nanoparticles compared to Al_2O_3, a rise in the TiO_2 ratio decreased the heat transfer coefficient, Nusselt number, and heat transfer rate. Inlet temperature was found to decrease pressure drop and performance index. The Al_2O_3 (5:0) nanofluid demonstrated the maximum enhancement of around 16.9%, 16.9%, 3.44%, and 3.41% for the heat transfer coefficient, Nusselt number, heat transfer rate, and performance index, respectively. Additionally, the TiO_2 (0:5) hybrid nanofluid exhibited enhancements of 0.61% and 2.3% for pressure drop and Prandtl number, respectively. The developed hybrid nanofluids enhanced the performance of the heat exchanger when used as a cold fluid.

Keywords: hybrid nanofluid; heat exchanger; particle ratio; performance index; thermal conductivity; viscosity

Citation: Bhattad, A.; Rao, B.N.; Atgur, V.; Veza, I.; Zamri, M.F.M.A.; Fattah, I.M.R. Thermal Performance Evaluation of Plate-Type Heat Exchanger with Alumina–Titania Hybrid Suspensions. *Fluids* **2023**, *8*, 120. https://doi.org/10.3390/fluids8040120

Academic Editor: D. Andrew S. Rees

Received: 13 March 2023
Revised: 28 March 2023
Accepted: 30 March 2023
Published: 2 April 2023

1. Introduction

Heat exchangers encounter several heat transfer issues during fluid flows. For this reason, industries have adopted the addition of nanoparticles to the working fluid to improve heat exchanger performance. Additives have been considered to enhance thermal properties [1–3]. Nanofluids are colloidal mixtures of base fluids and nano-sized particles (10–100 nm) [4,5]. Combining nanoparticles with base fluids makes it possible to improve thermal conductivity, density, viscosity, and specific heat, leading to enhanced heat transfer [6]. Nanofluids can be synthesised in a single or two-step process [7]. Due to their enhanced thermal conductivity, nanofluids find wide applications in various fields, such as heat exchangers [8], solar energy [9], refrigeration systems [10], and thermo-siphons [11]. The thermal conductivity of nanofluids can be measured using the 3-ω method, temperature oscillation, and transient hot-wire techniques [12–14]. The constants in models or empirical relationships utilised to evaluate nanofluids' thermal conductivity and viscosity are based on experimental data [15–23].

Researchers have recently focused on developing hybrid nanofluids to enhance thermal conductivity further [24]. Some studies have explored these hybrid solutions' preparation, characteristics, and heat transfer performance [25,26]. For instance, Qi et al. [27] studied the stability, thermal properties, and heat transfer behaviour of TiO_2 nanofluids. They found that surfactants are added to prevent the accumulation of nanoparticles in hybrid nanofluids [28]. Alkasmoul et al. [29] used TiO_2 and Al_2O_3-water nanofluids to cool a horizontal tube with constant heat flux, and they observed heat transfer degradation due to a decrease in Reynolds number for the same flow rate. Studies of water-based mono/hybrid nanofluids have shown that they can improve heat transfer characteristics and effectiveness in heat exchangers through energetic and exergetic performance analyses [30–34]. Hamid et al. [35] examined the thermal conductivity of hybrid nanofluids by dispersing TiO_2 and SiO_2 nanoparticles in the base fluid and reported a 16% increase in thermal conductivity. However, they also found that the 5:5 ratios of TiO_2/SiO_2 nanoparticles led to high viscosity. Charab et al. [36] established a nonlinear relation between thermal conductivity and particle concentration for Al_2O_3-TiO_2 hybrid nanofluids. Garud et al. [37] investigated the influence of different particles on the micro-plate heat exchanger. The oblate spheroid and platelet-shaped nanoparticles show superior and worse first and second law characteristics for Al_2O_3 and Al_2O_3/Cu nanofluids. Elias et al. [38] proposed a correlation for the thermal conductivity of hybrid nanofluids based on their shape function, finding that cylindrical particles outperformed other shapes. Various models have been proposed for hybrid nanofluid thermal conductivity [39–44] and a viscosity [19,41,45–48]. Hybrid nanofluids have also been found to improve the performance of plate heat exchangers (PHE) [49,50]. For instance, Maddah et al. [51] used Al_2O_3-TiO_2 hybrid nanofluids and observed enhanced exergetic efficiency. Hamid et al. [52] achieved heat transfer enhancement of up to 35.32% by mixing a 2:3 ratio of TiO_2/SiO_2 nanoparticles with the base fluid.

Based on previous investigations, limited research is available on evaluating the viscosity and thermal conductivity of Al_2O_3-TiO_2-water nanofluids and the thermal performance of plate heat exchangers (PHE) with hybrid nanofluids. Most studies have focused on the variation of nanoparticle concentration. In this study, the authors developed Al_2O_3-TiO_2 hybrid nanofluids with different particle volume ratios (0:5, 1:4, 2:3, 3:2, 4:1, and 5:0) at a concentration of 0.1% in deionised (DI) water. Experiments were conducted to evaluate the PHE performance with the developed hybrid nanofluids, examining the effects of varying particle volume ratios and fluid temperature (283 K-298 K) on various performance indicators. The authors also developed and verified thermal conductivity and viscosity evaluation models based on experimental data. Performance factors considered include the performance index (*PI*), heat transfer rate, heat transfer coefficient, Nusselt number, Prandtl number, and pressure drop.

This research aimed to investigate the effect of fluid temperature on the performance of a PHE using Al_2O_3-TiO_2 hybrid nanofluids with distinct particle volume ratios at a concentration of 0.1% in deionised water. To achieve this, suitable empirical relations were identified for the thermal conductivity and viscosity of the hybrid nanofluids. Experimental investigations were conducted on the PHE using the developed nanofluids to assess various performance indicators, including the performance index, heat transfer rate, Nusselt number, heat transfer coefficient, Prandtl number, and pressure drop.

2. Preparation and Characterization of Hybrid Nanofluids

A two-step method was followed for developing TiO_2-Al_2O_3-water hybrid nanofluid. The quantity of Al_2O_3 and TiO_2 nanoparticles was purchased and mixed in DI water. The mean size of Al_2O_3 and TiO_2 nanoparticles were 45 nm and 20 nm, respectively. Surfactant Span−80 was added to avoid particle accumulation in the hybrid solution.

Hybrid nanofluid prepared with TiO_2 and Al_2O_3 particles of distinct ratios (0:5, 1:4, 2:3, 3:2, 4:1, and 5:0) with 0.1 v%. Equation (1) depicts the volume fractions of solids in the fluid.

$$\phi = \left\{ \left(\frac{m}{\rho}\right)_{p1} + \left(\frac{m}{\rho}\right)_{p2} \right\} \left\{ \left(\frac{m}{\rho}\right)_{p1} + \left(\frac{m}{\rho}\right)_{p2} + \left(\frac{m}{\rho}\right)_{bf} \right\}^{-1} \quad (1)$$

Here ρ (kg/m^3) is the density. ϕ is the solid volume fraction. m (kg) is the mass.

SEM (Scanning electron microscopy) and TEM (Transmission electron microscopy) tests were performed and measured the mean size of Al_2O_3 and TiO_2 nanoparticles by ImageJ software 2.0.0-rc-3 (https://imagej.net/imaging/particle-analysis) (accessed on 27 March 2023) as 45 nm and 20 nm, respectively. The small-size particles in Figure 1 represent TiO_2 nanoparticles, whereas larger ones are the Al_2O_3 nanoparticles. Both types of nanoparticles were found to be spherical, with a shape factor of 1. One of the key challenges in studying nanofluids is ensuring their stability and homogeneity. A stability test involving gravitational settling was performed to address this issue, and images of the test tube were taken at different intervals (Figure 2). The results showed that there was no sedimentation throughout the 7-day investigation.

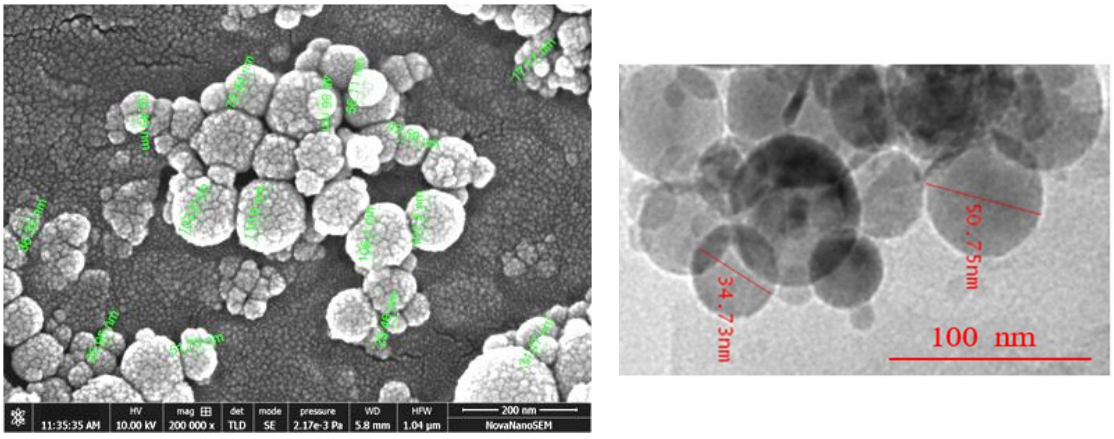

(**a**) (**b**)

Figure 1. (**a**). SEM image of Al_2O_3- TiO_2/water hybrid nanofluid; (**b**). TEM image of Al_2O_3-TiO_2/water hybrid nanofluid.

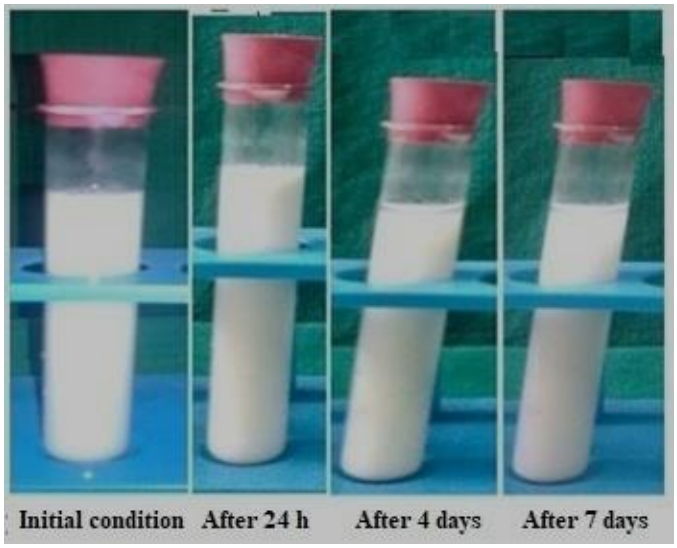

Figure 2. Stability analysis of a sample showing no sedimentation for 7 days.

The Hot Disk Thermal Constants Analyser (Figure 3) used the Transient Plane Source technique to measure the thermal conductivity of the base fluids, mono-nanofluid, and hybrid nanofluid with an accuracy of ±1.5%. The specific heat was also measured using the same device. The fluid density was determined by weighing the mass and volume of the liquid using a digital weighing machine. Repeated measurements were conducted to confirm consistency in the results. The DV1 Brookfield digital viscometer (Figure 4), with an accuracy of ±1.0%, was utilized to measure the viscosity of the base fluids, mono-nanofluid, and hybrid nanofluid. The viscometer operates by driving a plate immersed in the test sample, and the viscous force of the fluid was calculated using the measured spring deflection with 1.0 mL of fluid. The operative mechanism of the viscometer is to drive the plate immersed in the test sample. The viscous force of the fluid was evaluated from the measured spring deflection with the help of 1.0 mL of fluid.

Figure 3. Hot disk thermal constants analyser.

Figure 4. Brookfield digital viscometer.

3. Performance of PHE with Hybrid Nanofluid

Experimental investigations were carried out on plate heat exchangers (PHE) using Al_2O_3-TiO_2/Water-based binary nanofluid developed in-house. The performance parameters evaluated in the experiments included the performance index, heat transfer rate, heat transfer coefficient, Prandtl number, Nusselt number, and pressure drop. Figure 5 shows

the experimental setup. The red arrow in Figure 5 shows the PHE, whose specifications are well described in earlier research [50].

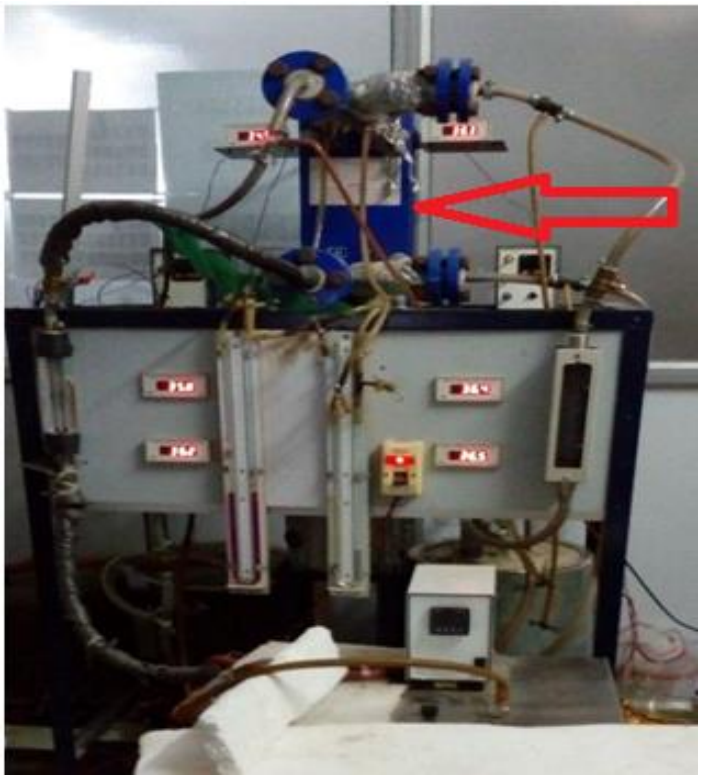

Figure 5. Experimental setup showing PHE with a red arrow.

The investigation employed a commercial PHE manufactured by Alfa Laval India Limited as the test section, which had an effective heat transfer area of 0.3 m^2, was made of SA 240 GR.316 stainless steel material, and had a plate thickness of 0.5 mm. The experimental setup included separate hot and cold fluid circuits. The hot circuit comprised an insulated tank with an immersion heater to maintain the desired inlet temperature of the hot fluid, a float-type flowmeter, a manometer, and a hot fluid pump. The tank contained DI water, which was heated and then pumped to the heat exchanger through a flowmeter to measure the fluid flow rate. The cold circuit consisted of an isothermal bath, a float flowmeter, a manometer, and a plate heat exchanger. A hybrid nanofluid was stored in the isothermal bath and cooled to maintain a constant inlet temperature of the cold fluid, which was then pumped to the plate heat exchanger via a flowmeter. Thermocouples were placed at the inlet and outlet of both hot and cold fluid streams to measure their temperatures, and a U-tube type differential manometer was used to measure the pressure difference between the inlet and outlet of the fluids. The pipes were insulated to minimise heat exchange with the surroundings. Once the inlet temperatures and flow rates of the hot and cold fluids were set, all the measuring parameters were recorded at the steady state condition.

Experiments considered DI water and hybrid solution as the hot and cold fluids, respectively. Heat transfer between a hot liquid (Q_h) and a cold liquid (Q_c) is evaluated from Equations (2) and (3):

$$Q_h = \dot{m}_h C_{ph}(T_{hi} - T_{ho}) \tag{2}$$

and

$$Q_c = \dot{m}_{nf} C_{pnf}(T_{co} - T_{ci}) \tag{3}$$

Experiments were conducted, keeping the hot inlet temperature (T_{hi}) at 35 °C, and varying the cold inlet temperature (T_{ci}) between 10 °C and 25 °C with a 3 lpm mass flow rate of both side fluids. LMTD (logarithmic mean temperature difference) value obtained

from the measured temperature at terminal points. The hybrid nanofluid heat transfer coefficient (α_c) was obtained from the overall heat transfer coefficient (U) and hot water heat transfer coefficient (α_h).

$$\frac{1}{U} = \frac{1}{\alpha_h} + \frac{1}{\alpha_c} + \frac{t}{k_w} = \frac{A}{Q} \times LMTD \tag{4}$$

Here, kw represents the thermal conductivity of the plate material, and (in W/m-K) is the plate thickness (in mm). Q is the heat transfer rate (in W). A is surface area = 0.3 m^2.

The hot water heat transfer coefficient (α_h) evaluated from the Nusselt number [53]:

$$Nu = 0.2594\mathrm{Re}^{0.76}\mathrm{Pr}^{0.3} \tag{5}$$

The Nusselt number (Nu) and the Prandtl number (Pr) for hybrid nanofluids obtained from

$$Nu = \frac{\alpha D_h}{k} \tag{6}$$

$$\mathrm{Pr} = \frac{\mu c_p}{k} \tag{7}$$

The pressure drop (Δp) was recorded during experiments. Assuming 80% pump efficiency [54], the performance index (PI) of PHE with hybrid nanofluids obtained from

$$PI = \frac{0.8\rho_{nf}Q}{\Delta p_{nf} m_{nf}} \tag{8}$$

4. Uncertainty Study

Different parameters were measured using appropriate instruments during experimentation. The uncertainty in the parameters was estimated using Equation (9) [55].

$$\frac{\delta X}{X} = \sqrt{\left[\left(\frac{\delta x_1}{x_1}\right)^2 + \left(\frac{\delta x_2}{x_2}\right)^2 + - - - - + \left(\frac{\delta x_n}{x_n}\right)^2\right]} \tag{9}$$

The estimated uncertainties are discussed in the Results and Discussion section.

5. Results and Discussion

This section describes the measured thermo-physical properties and post processing data based on primary data, empirical formulas to determine a hybrid nanofluid's thermal conductivity, and viscosity. Moreover, the performance analysis of PHE is also discussed. Table 1 displays the thermo-physical properties (including thermal conductivity (k_{bf}), density (ρ_{bf}), viscosity (μ_{bf}), specific heat (C_{Pbf}), and the Prandtl number (Pr_{bf})) measured using instruments with various temperatures (T) for the base fluid (DI Water), nanofluid, and hybrid nanofluid.

Table 1. (**a**). Thermo-physical properties of DI water. (**b**). Thermo-physical properties of hybrid nanofluids.

(**a**)

T (K)	k_{bf} (W/m-K)	ρ_{bf} (kg/m^3)	μ_{bf} (mPa·S)	C_{Pbf} (J/kg·K)	Pr_{bf}
283	0.5823	997.8	0.9549	4183	6.774
288	0.5896	996.8	0.8706	4183	6.106
293	0.5964	996.0	0.8150	4183	5.668
298	0.6014	994.7	0.7493	4183	5.157

Table 1. *Cont.*

T (K)	(b) Al_2O_3–TiO_2–WaterNanofluids					
	TiO_2(0:5)	Hybrid (1:4)	Hybrid (2:3)	Hybrid (3:2)	Hybrid (4:1)	Al_2O_3(5:0)
	Thermal Conductivity, k_{hnf} (W/m-K)					
283	0.5919	0.5921	0.5921	0.5921	0.5922	0.5922
288	0.5979	0.5993	0.5993	0.5994	0.5994	0.5994
293	0.6036	0.6046	0.6046	0.6047	0.6047	0.6047
298	0.6091	0.6100	0.6101	0.6109	0.6109	0.6109
	Density, ρ_{hnf} (kg/m^3)					
283	1001.0	1000.9	1000.9	1000.8	1000.8	1000.7
288	1000.0	999.7	999.7	999.6	999.6	999.5
293	999.0	998.8	998.7	998.7	998.7	998.6
298	997.9	997.7	997.6	997.4	997.4	997.3
	Viscosity, μ_{hnf} (mPa·S)					
283	0.9684	0.9684	0.9684	0.9684	0.9684	0.9684
288	0.8935	0.8786	0.8786	0.8786	0.8786	0.8786
293	0.8275	0.8187	0.8187	0.8187	0.8187	0.8187
298	0.7690	0.7612	0.7612	0.7535	0.7535	0.7535
	Specific Heat, C_{phnf} (J/kg·K)					
283	4169	4169	4169	4169	4169	4169
288	4169	4169	4169	4169	4169	4170
293	4169	4169	4169	4169	4169	4170
298	4168	4169	4169	4169	4169	4170
	Prandtl Number, Pr_{hnf}					
283	6821	6819	6819	6819	6817	6817
288	6230	6112	6112	6111	6111	6112
293	5715	5645	5645	5644	5644	5646
298	5262	5202	5202	5142	5142	5143

5.1. Empirical Relation for Thermal Conductivity

In the first step, the thermal conductivity of the samples was measured through experiments. The adequacy of the Corcione model [19] was then verified by modifying it with the obtained test data. Following this, hybrid nanofluid was prepared by dispersing alumina and titania nanoparticles in the base fluid. Different suspensions of 0.1 v% composition, with varying ratios (5:0, 4:1, 3:2, 2:3, 1:4, and 0:5) of alumina and titania nanoparticles, were tested for the specific temperature range (from 283 K to 298 K). Defining ϕ_1 and ϕ_2 are the concentrations of alumina and titania nanoparticles. $\phi = \phi_1 + \phi_2$, is the concentration of the hybrid nanocomposites. The modified Corcione model for thermal conductivity is:

$$k_{hnf} = k_{bf}\left\{1 + f_k \mathrm{Re}^{0.4}\mathrm{Pr}^{0.66}\left(\frac{T}{T_{fr}}\right)^{10}\left(\frac{k_p}{k_{bf}}\right)^{0.03}\phi^{0.66}\right\} \quad (10)$$

Corcione [19] suggested the constant, f_k = 4.4, in Equation (10), whereas in the present study, f_k =8.8. The reference temperature, $T_{fr} = 284$ K. T is the working temperature. Re = $\frac{\rho_{bf} k_B T}{\pi r_p \mu_{bf}^2}$, is the Reynolds number. Pr is the Prandtl number. Thermal conductivity of the nanoparticles, $k_p = \frac{\phi k_{p1} k_{p2}}{\phi_1 k_{p2} + \phi_2 k_{p1}}$. The equivalent radius of nanoparticles, $r_p = \left(\frac{\phi_1 r^3{}_1 + \phi_2 r^3{}_2}{\phi_1 + \phi_2}\right)^{\frac{1}{3}}$. Boltzmann constant, $k_B = 1.3807 \times 10^{-23}$.

Table 2 displays the experimental thermal conductivity results for 0.1 v% Al_2O_3 and TiO_2 nanofluids with temperature. The modified Corcione model (10) agrees with the experimental data. In a study by Tiwari et al. [55], thermal conductivity data of Al_2O_3 nanofluids at 323 K for different concentrations were generated, and the modified Corcione model (10) was found to be reasonably accurate in predicting the data, as shown in Table 3. The modified Corcione model (10) predicts thermal conductivity well for low and high concentrations of Al_2O_3 nanofluids. A comparison of estimates with test data of thermal conductivity for the developed hybrid suspensions is shown in Table 4. The hybrid nanofluids exhibit higher thermal conductivity than the base fluid, with slightly lower thermal conductivity for titanianofluids than for alumina nanofluids. Thus, the thermal conductivity of the solution is enhanced when the alumina contribution is higher in the solution. The thermal conductivity (Figure 6) increases with temperature, which is significant at high temperatures due to the Brownian effect. The experiments were conducted multiple times to ensure the measured data's repeatability, and the data's variation at each data point was represented using error bars.

Table 2. Thermal conductivity for Al_2O_3 and TiO_2 nanofluids (0.1 v%) with temperature.

T (K)	Thermal Conductivity (W/m·K)					
	Al_2O_3 Nanofluid			TiO_2 Nanofluid		
	Test	f_k = 4.4 in Equation (10)	f_k = 8.8 in Equation (10)	Test	f_k = 4.4 in Equation (10)	f_k = 8.8 in Equation (10)
283	0.5922	0.5840	0.5858	0.5919	0.5836	0.5850
288	0.5994	0.5917	0.5939	0.5979	0.5912	0.5929
293	0.6047	0.5990	0.6016	0.6029	0.5983	0.6003
298	0.6109	0.6045	0.6077	0.6089	0.6038	0.6061

Table 3. Thermal conductivity data of Al_2O_3 nanofluid at 323 K for different concentrations.

Concentration (ϕ)	Thermal Conductivity (W/m·K)		Concentration (ϕ)	Thermal Conductivity (W/m·K)	
	Test [56]	f_k = 8.8 in Equation (10)		Test [56]	f_k = 8.8 in Equation (10)
0.005	0.6884	0.6953	0.035	0.8400	0.8408
0.010	0.7232	0.7276	0.040	0.8590	0.8593
0.015	0.7484	0.7546	0.045	0.8779	0.8771
0.020	0.7737	0.7787	0.050	0.8969	0.8942
0.025	0.7990	0.8007	0.055	0.9127	0.9107
0.030	0.8179	0.8213	0.060	0.9285	0.9268

Table 4. Thermal conductivity of hybrid nanofluids at different temperatures and particle ratio.

Fluid	Temperature, T (K)			
	283	288	293	298
DI Water	0.5896	0.5964	0.6014	0.6077
TiO_2 (0:5)	0.5919	0.5979	0.6029	0.6089
Hybrid (1:4)	0.5920	0.5983	0.6031	0.6094
Hybrid (2:3)	0.5921	0.5985	0.6035	0.6098
Hybrid (3:2)	0.5921	0.5987	0.6039	0.6102
Hybrid (4:1)	0.5922	0.5992	0.6043	0.6106
Al_2O_3 (5:0)	0.5922	0.5994	0.6047	0.6109

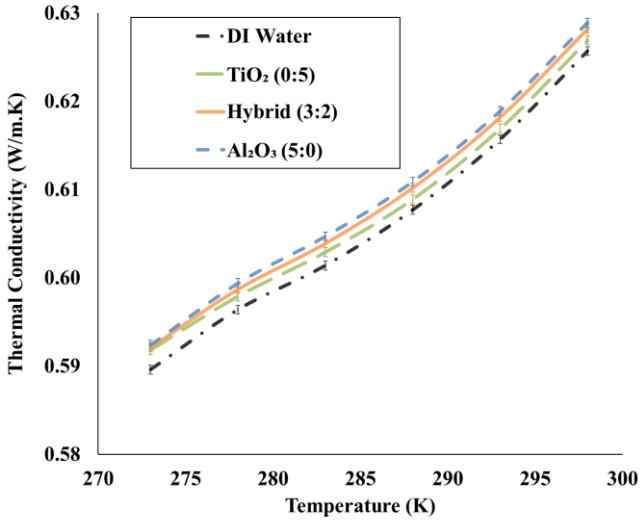

Figure 6. Thermal conductivity versus temperature for different fluids.

The thermal conductivity of the hybrid nanofluid was modelled using the modified Corcione model (model 2), which considers the temperature, volume fraction, thermal conductivity and size of nanoparticles, and the base fluid thermal conductivity. The comparison between the measured and estimated thermal conductivity for hybrid nanofluid is presented in Figure 7. Based on the superposition principle, the model proposed by Eid and Nafe [57] gave low values for the thermal conductivity of a hybrid nanofluid. On the other hand, the modified Corcione model demonstrated an average deviation of only 0.3% between the test data and estimated values.

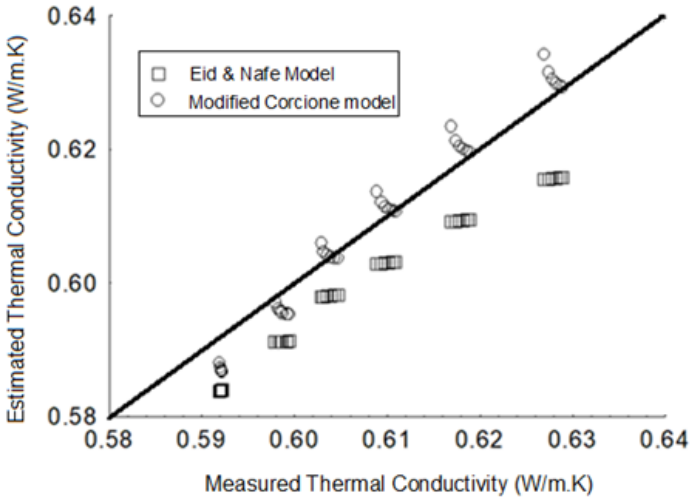

Figure 7. Comparison of measured and estimated thermal conductivity for hybrid nanofluid.

5.2. Empirical Relation for Effective Viscosity

The modified Corcione model for effective viscosity (μ_{eff}) of hybrid nanofluid is:

$$\mu_{eff} = \mu_{bf}\left\{1 - 27.02\left(\frac{d_p}{d_{bf}}\right)^{-0.3}\phi^{1.03}\right\}^{-1} \quad (11)$$

Here,

$d_{bf} = \sqrt[3]{\frac{0.006M}{\pi N(\rho_{bf})_0}}$, represents the equivalent diameter of a fluid molecule; $M = 18.0152891$ moles, represents the molecular weight of the fluid; $N = 6.022 \times 10^{23}$, represents the Avo-

gadro number; and $\left(\rho_{bf}\right)_0 = 998$ kg/m^3, describes the mass density of the base fluid at temperature $d_p = 2r_p$, represents the particle diameter.

The measured viscosity of alumina (Al_2O_3) nanofluid and titania (TiO_2) nanofluid for different concentrations and temperatures are presented in Table 5. Estimates from Equation (11) match the test data with a 1.5% deviation. Estimates from Equation (11) and Tiwari et al. [55] test data for different particle concentrations at 323 K in Table 6 have a 2% deviation. The effective viscosity of the hybrid nanofluid (Table 7) is more than the base fluid. Due to high titania particle viscosity, titania nanofluid is high, and alumina nanofluid is low.

Table 5. Effective viscosity (μ_{eff}) of Al_2O_3 and TiO_2 nanofluids (0.1 v%) with temperature.

Temperature, T (K)	Effective Viscosity, μ_{eff} (mPa·s)			
	Al_2O_3 Nanofluid Model 3		TiO_2 Nanofluid	
	Test	Equation (3)	Test	Equation (3)
283	0.9684	0.9600	0.9684	0.9614
288	0.8786	0.8753	0.8935	0.8766
293	0.8187	0.8194	0.8275	0.8206
298	0.7535	0.7533	0.7690	0.7544

Table 6. Effective viscosity (μ_{eff}) of Al_2O_3 nanofluid (0.1 v%) at 323 K varying concentration (ϕ).

Concentration, ϕ	Effective Viscosity, μ_{eff} (mPa·s)	
	Test [50,53]	Equation (3)
0.005	0.5467	0.5536
0.010	0.5596	0.5706
0.015	0.5763	0.5891
0.020	0.5973	0.6089
0.025	0.6220	0.6304
0.030	0.6511	0.6536
0.035	0.6839	0.6786
0.040	0.7211	0.7058

Table 7. Effective viscosity (μ_{eff}) of hybrid nanofluid having different particle ratios at a specific temperature.

Fluid	Effective Viscosity, μ_{eff} (mPa·s)			
	Temperature, T (K)			
	283	288	293	298
DI Water	0.9549	0.8706	0.8150	0.7493
TiO_2 (0:5)	0.9707	0.8850	0.8285	0.7617
Hybrid (1:4)	0.9690	0.8835	0.8271	0.7604
Hybrid (2:3)	0.9683	0.8828	0.8264	0.7598
Hybrid (3:2)	0.9679	0.8824	0.8261	0.7595
Hybrid (4:1)	0.9675	0.8821	0.8258	0.7592
Al_2O_3 (5:0)	0.9673	0.8819	0.8256	0.7590

Estimated and measured effective viscosity (μ_{eff}) for alumina nanofluid and titania nanofluid are in agreement. In the case of a hybrid nanofluid, Equation (11) is used, replacing the particle size with an adequate size of the hybrid nanofluid. Figure 8 illustrates that the estimated viscosity had an average deviation of 0.8% from the measured viscosity. The error bar on the graph depicts the variability and repeatability of the experimental data.

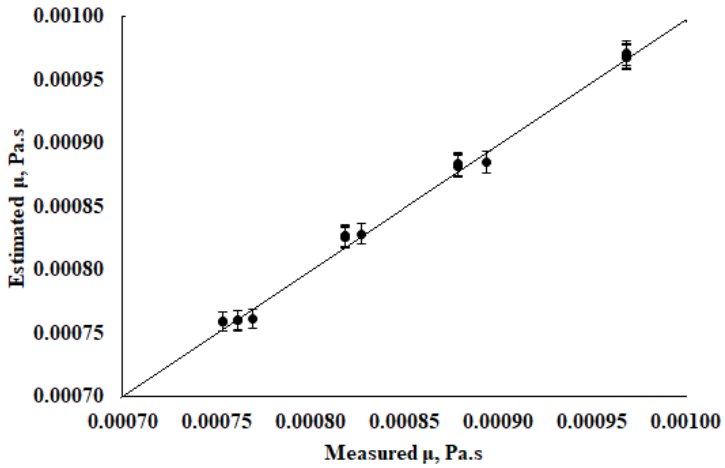

Figure 8. Estimated and measured effective viscosity, (Pa·s) of hybrid nanofluid.

Empirical relations for density and specific heat of hybrid nanofluid are [43]:

$$\rho_{hnf} = \phi_1 \rho_{p1} + \phi_2 \rho_{p2} + (1 - \phi)\rho_{bf} \quad (12)$$

$$\rho_{hnf} C_{Phnf} = \phi_1 \rho_{p1} C_{P1} + \phi_2 \rho_{p2} C_{P2} + (1 - \phi) \rho_{bf} C_{Pbf} \quad (13)$$

5.3. Experimental Results

Experiments were conducted on a plate heat exchanger (PHE) with coolant as a hybrid nanofluid and hot fluid as DI water. Hybrid nanofluids were prepared by suspending TiO_2 and Al_2O_3 nanoparticles in ratios, 5:0, 4:1, and so on till 0:5, to a base fluid (DI water) at 0.1 v% for the specific operating temperature (varying from 283 K to 298 K). The hot fluid inlet temperature and flow rate were 35 °C (308 K) and 3 lpm, respectively. Factors determined for performance assessment of PHE were heat transfer rate (Q), heat transfer coefficient (α_{nf}), Nusselt number (Nu_{nf}), Prandtl number (Pr_{nf}), pressure drop (Δp_c), and performance index (PI).

Table 8 provides the recorded outlet temperature of cold (T_{co}) and hot (T_{ho}) liquids. Thermo-physical properties of fluids at 25 °C are in Table 9. These recorded data are used for the calculation of heat transfer rate (Q), heat transfer coefficient (αnf), Nusselt number (Nu_{nf}), Prandtl number (Pr_{nf}), pressure drop (Δp_c), and performance index (PI).

Table 8. Recorded cold and hot fluids outlet temperature keeping the hot inlet temperature (T_{hi}) at 35 °C and varying the cold inlet temperature (T_{ci}).

Fluid	Outlet Temperature, T_{co} (°C) of the Cold Fluid				Outlet Temperature, T_{ho} (°C) of the Hot Fluid			
	Cold Inlet Temperature, T_{ci} (°C)				Cold Inlet Temperature, T_{ci} (°C)			
	10	15	20	25	10	15	20	25
DI water	23.55	26.20	28.85	30.95	21.42	23.81	26.44	28.95
TiO_2 (0:5)	23.65	26.32	29.06	31.15	21.40	23.72	26.39	28.91
Hybrid (1:4)	23.68	26.37	29.10	31.28	21.39	23.69	26.37	28.89
Hybrid (2:3)	23.72	26.44	29.18	31.41	21.37	23.66	26.35	28.87
Hybrid (3:2)	23.76	26.53	29.27	31.50	21.35	23.63	26.33	28.85
Hybrid (4:1)	23.79	26.61	29.35	31.59	21.33	23.60	26.31	28.83
Al_2O_3 (5:0)	23.82	26.69	29.43	31.68	21.31	23.59	26.30	28.82

Table 9. Thermo-physical properties of fluids at 25 °C.

	***Cp* (J/kg·K)**	***k* (W/m·K)**	**ρ (kg/m^3)**	**μ (mPa·s)**
DI water	4183	0.6077	994.7	0.7493
TiO_2 (0:5)	4169	0.6136	997.9	0.7544
Hybrid (1:4)	4169	0.6120	997.7	0.7538
Hybrid (2:3)	4169	0.6114	997.6	0.7536
Hybrid (3:2)	4169	0.6110	997.4	0.7535
Hybrid (4:1)	4169	0.6108	997.4	0.7534
Al_2O_3 (5:0)	4170	0.6107	997.3	0.7533

The uncertainties estimated from equation 9 are 2.1%, 2.0%, 3.9%, 4.5%, 0.1%, and 1.2% in the performance index, heat transfer rate, convective heat transfer coefficient, Nusselt number, pressure drop, and Prandtl number, respectively.

The results of performance parameters with hybrid nanofluids at a constant flowing rate of 3 lpm and varying inlet temperatures (283 K to 298 K) are presented in Table 10. As expected, the heat transfer rate decreases with the inlet temperature of the cold fluid, whereas the addition of hybrid nanofluids increases the heat transfer rate. Specifically, the Al_2O_3 and TiO_2 particle combination with a ratio of 5:0 (Al_2O_3 (5:0)) shows an augmentation in the heat transfer rate of 3.44%. This improvement is attributed to the higher thermal conductivity of solid particles compared to the base fluid, resulting in an overall enhancement of the thermal conductivity of the solution. Moreover, since the thermal conductivity of alumina is greater than that of titania nanoparticles, Al_2O_3 (5:0) fluid offers the maximum heat transfer rate.

Furthermore, an investigation was conducted to determine the heat transfer coefficient of the fluid. The results indicate that the combination of Al_2O_3 (5:0) offers the best performance, with an improvement of 16.9% in the heat transfer coefficient. This finding can be attributed to this fluid's high thermal conductivity and heat transfer rate, leading to an elevated heat transfer coefficient. In addition, the Nusselt number was found to have increased by 16.9% for the Al_2O_3 (5:0) nanofluid. The Nusselt number is directly related to the heat transfer coefficient. Consequently, since the heat transfer coefficient is highest for the Al_2O_3 (5:0) nanofluid and lowest for water, the Nusselt number behaves similarly. Furthermore, the heat transfer coefficient and Nusselt number increase with an increase in the inlet temperature of the fluid.

The decrease in the inlet temperature of the coolant led to a reduction in pressure drop, whereas hybrid nanofluids caused an increase in pressure drop. Among the hybrid nanofluids, TiO_2 (0:5) showed the highest pressure drop with a negligible increase of 0.6%. The addition of nanoparticles increased pressure drop due to the mass-volume ratio. The fluid with the highest mass-volume ratio exhibited the maximum pressure drop.

Using hybrid nanofluids with high heat capacity improved the heat transfer coefficient and heat transfer rate. However, the increase in viscosity resulted in a higher pressure drop. The Performance Index (*PI*) was utilized as a criterion to compare the enhancement in heat transfer rate and pump work. The results showed that adding nanoparticles to the base fluid increased both factors. The *PI*, defined as the heat transfer rate and pressure drop ratio, was highest for the Al_2O_3 (5:0) nanofluid, indicating that the heat transfer rate improvement was greater than the pump work increase. The *PI* increased by 3.41%.

It was observed that the Prandtl number reduces with a rise in the temperature. Furthermore, it was enhanced with the addition of nanoparticles in the primary fluid. It was increased by around 2.3% for the titania nanofluid (TiO_2 (0:5)) case because viscosity is higher and thermal conductivity is less for titania than alumina nanofluid. Moreover, the Prandtl number is a viscosity and thermal conductivity ratio. The improved performance characteristics of hybrid nanofluids make them a superior preference for industrial applications.

Table 10. Performance parameters varying coolant inlet temperature from 283 K to 298 K.

	Heat Transfer Rate, Q (kW)				**Pressure Drop, Δp_c (Pa)**			
	283 K	**288 K**	**293 K**	**298 K**	**283 K**	**288 K**	**293 K**	**298 K**
DI water	2833.983	2342.48	1790.978	1264.443	315.01	310.46	305.5	300.4
TiO_2 (0:5)	2845.343	2359.654	1810.557	1281.66	316.25	311.5	307.4	302.6
Hybrid (1:4)	2851.596	2360.077	1812.895	1286.066	316.16	311.31	307.21	302.42
Hybrid (2:3)	2859.934	2372.668	1818.571	1289.165	316	311.09	307.13	302.26
Hybrid (3:2)	2868.272	2378.429	1832.332	1295.925	315.9	310.89	306.78	302.1
Hybrid (4:1)	2869.526	2390.105	1839.008	1301.686	315.76	310.75	306.53	301.84
Al_2O_3 (5:0)	2870.779	2407.365	1848.155	1307.78	315.64	310.64	306.38	301.61
	Nusselt number, Nu_{nf}				Prandtl number, Pr_{nf}			
DI water	10.116	11.056	12.274	14.353	6775	6106	5645	5143
TiO_2 (0:5)	10.192	11.351	12.683	14.997	6821	6158	5715	5262
Hybrid (1:4)	10.248	11.400	12.767	15.112	6819	6116	5669	5244
Hybrid (2:3)	10.333	11.597	12.984	15.368	6819	6115	5665	5225
Hybrid (3:2)	10.418	11.763	13.350	15.760	6818	6114	5661	5204
Hybrid (4:1)	10.455	11.969	13.620	16.169	6817	6113	5658	5182
Al_2O_3 (5:0)	10.484	12.209	13.898	16.713	6817	6111	5656	5158
	Heat transfer coefficient, α_{nf} (W/m^2.K)				Performance Index, PI			
DI water	1217.26	1345.69	1506.43	1780.02	549.49	454.39	347.58	245.51
TiO_2 (0:5)	1231.13	1385.00	1562.34	1864.27	551.72	457.67	351.31	248.80
Hybrid (1:4)	1238.34	1394.31	1575.24	1881.25	552.84	457.76	351.77	249.66
Hybrid (2:3)	1248.58	1418.40	1602.10	1913.42	554.47	460.22	352.88	250.27
Hybrid (3:2)	1258.94	1438.95	1647.46	1964.82	556.09	461.34	355.56	251.58
Hybrid (4:1)	1263.59	1464.10	1680.88	2015.89	556.34	463.61	356.86	252.71
Al_2O_3 (5:0)	1267.07	1493.51	1715.09	2083.64	556.59	466.97	358.64	253.90

6. Conclusions

The heat transfer performance of a plate-type heat exchanger (PHE) primarily depends on thermal properties such as thermal conductivity. To enhance thermal conductivity, nanoparticles are introduced into the base fluid. This study presents empirical models for determining the thermal conductivity and viscosity of TiO_2–Al_2O_3/water hybrid nanofluids by modifying the Corcione empirical relations with measured data. These models can estimate binary and mono nanofluids' thermal conductivity and viscosity.

Additionally, the heat transfer characteristics of Al_2O_3-TiO_2 hybrid nanofluid were investigated in a plate-type heat exchanger. The experiments were performed at various particle ratios and inlet temperatures, using a 0.1% volume concentration. The results of the investigation are presented below:

- The Al_2O_3-TiO_2/water-based hybrid nanofluids performed better than DI water. However, as the concentration of TiO_2 particles in the solution increased, the heat transfer coefficient and the heat transfer rate decreased. An improvement of 16.9% in heat transfer coefficient, 16.9% in Nusselt number, and 3.44% in heat transfer rate were observed with 0.1% volume concentration of Al_2O_3/water nanofluid;
- Pressure drop reduces with inlet temperature. A total of 0.61% enhancement was observed in the pump work for 0.1 v% TiO_2-water nanofluid;
- The Prandtl number was observed to be highest for TiO_2-water nanofluid with an enhancement of 2.3%;
- An increase in the inlet temperature results in a reduction in the performance index, whereas the use of hybrid nanofluids leads to its improvement. The alumina nanofluid showed an enhancement of 3.41% in the performance index;
- The use of hybrid nanofluids as coolants in plate heat exchangers improved their performance. Among the studied fluids, the alumina nanofluid performed better in most cases.

Author Contributions: Conceptualization, A.B.; Data curation, V.A. and M.F.M.A.Z.; Formal analysis, A.B.; Funding acquisition, I.M.R.F.; Investigation, A.B.; Methodology, A.B.; Project administration, B.N.R.; Resources, B.N.R., I.V. and M.F.M.A.Z.; Supervision, B.N.R.; Visualization, I.V.; Writing—original draft, A.B., V.A. and I.M.R.F.; Writing—review and editing, A.B., B.N.R., V.A., I.V., M.F.M.A.Z. and I.M.R.F. All authors have read and agreed to the published version of the manuscript.

Funding: This research was funded by 'University of Technology Sydney' through 'Strategic Research Support' funding with grant number [2200034].

Data Availability Statement: The data presented in this study are available on request from the corresponding author.

Acknowledgments: The authors wish to acknowledge Jahar Sarkar of IIT BHU Varanasi, India, for providing testing facilities to conduct the investigations.

Conflicts of Interest: The authors declare no conflict of interest.

References

1. Rostami, S.; Shahsavar, A.; Kefayati, G.; Shahsavar Goldanlou, A. Energy and Exergy Analysis of Using Turbulator in a Parabolic Trough Solar Collector Filled with Mesoporous Silica Modified with Copper Nanoparticles Hybrid Nanofluid. *Energies* **2020**, *13*, 2946. [CrossRef]
2. Ejaz, A.; Babar, H.; Ali, H.M.; Jamil, F.; Janjua, M.M.; Fattah, I.M.R.; Said, Z.; Li, C. Concentrated photovoltaics as light harvesters: Outlook, recent progress, and challenges. *Sustain. Energy Technol. Assess.* **2021**, *46*, 101199. [CrossRef]
3. Mofijur, M.; Siddiki, S.Y.A.; Shuvho, M.B.A.; Djavanroodi, F.; Fattah, I.M.R.; Ong, H.C.; Chowdhury, M.A.; Mahlia, T.M.I. Effect of nanocatalysts on the transesterification reaction of first, second and third generation biodiesel sources-A mini-review. *Chemosphere* **2021**, *270*, 128642. [CrossRef] [PubMed]
4. Choi, S.U.S.; Eastman, J.A. Enhancing thermal conductivity of fluids with nanoparticles. In Proceedings of the International Mechanical Engineering Congress and Exhibition, San Francisco, CA, USA, 12–17 November 1995.
5. Razzaq, L.; Mujtaba, M.A.; Soudagar, M.E.M.; Ahmed, W.; Fayaz, H.; Bashir, S.; Fattah, I.M.R.; Ong, H.C.; Shahapurkar, K.; Afzal, A.; et al. Engine performance and emission characteristics of palm biodiesel blends with graphene oxide nanoplatelets and dimethyl carbonate additives. *J. Environ. Manag.* **2021**, *282*, 111917. [CrossRef]
6. Das, P.K. A review based on the effect and mechanism of thermal conductivity of normal nanofluids and hybrid nanofluids. *J. Mol. Liq.* **2017**, *240*, 420–446. [CrossRef]
7. Azmi, W.H.; Sharma, K.V.; Mamat, R.; Najafi, G.; Mohamad, M.S. The enhancement of effective thermal conductivity and effective dynamic viscosity of nanofluids—A review. *Renew. Sustain. Energy Rev.* **2016**, *53*, 1046–1058. [CrossRef]
8. Chen, T.; Kim, J.; Cho, H. Theoretical analysis of the thermal performance of a plate heat exchanger at various chevron angles using lithium bromide solution with nanofluid. *Int. J. Refrig.* **2014**, *48*, 233–244. [CrossRef]
9. Khan, J.A.; Mustafa, M.; Hayat, T.; Farooq, M.A.; Alsaedi, A.; Liao, S.J. On model for three-dimensional flow of nanofluid: An application to solar energy. *J. Mol. Liq.* **2014**, *194*, 41–47. [CrossRef]
10. Sözen, A.; Özbaş, E.; Menlik, T.; Çakır, M.T.; Gürü, M.; Boran, K. Improving the thermal performance of diffusion absorption refrigeration system with alumina nanofluids: An experimental study. *Int. J. Refrig.* **2014**, *44*, 73–80. [CrossRef]
11. Buschmann, M.H.; Franzke, U. Improvement of thermosyphon performance by employing nanofluid. *Int. J. Refrig.* **2014**, *40*, 416–428. [CrossRef]
12. Das, S.K.; Putra, N.; Thiesen, P.; Roetzel, W. Temperature Dependence of Thermal Conductivity Enhancement for Nanofluids. *J. Heat Transf.* **2003**, *125*, 567–574. [CrossRef]
13. Oh, D.-W.; Jain, A.; Eaton, J.K.; Goodson, K.E.; Lee, J.S. Thermal conductivity measurement and sedimentation detection of aluminum oxide nanofluids by using the 3ω method. *Int. J. Heat Fluid Flow* **2008**, *29*, 1456–1461. [CrossRef]
14. Timofeeva, E.V.; Gavrilov, A.N.; McCloskey, J.M.; Tolmachev, Y.V.; Sprunt, S.; Lopatina, L.M.; Selinger, J.V. Thermal conductivity and particle agglomeration in alumina nanofluids: Experiment and theory. *Phys. Rev. E* **2007**, *76*, 061203. [CrossRef] [PubMed]
15. Batchelor, G.K. The effect of Brownian motion on the bulk stress in a suspension of spherical particles. *J. Fluid Mech.* **1977**, *83*, 97–117. [CrossRef]
16. Berger Bioucas, F.E.; Rausch, M.H.; Schmidt, J.; Bück, A.; Koller, T.M.; Fröba, A.P. Effective Thermal Conductivity of Nanofluids: Measurement and Prediction. *Int. J. Thermophys.* **2020**, *41*, 55. [CrossRef]
17. Brinkman, H.C. The Viscosity of Concentrated Suspensions and Solutions. *J. Chem. Phys.* **1952**, *20*, 571. [CrossRef]
18. Chandrasekar, M.; Suresh, S.; Chandra Bose, A. Experimental investigations and theoretical determination of thermal conductivity and viscosity of Al_2O_3/water nanofluid. *Exp. Therm. Fluid Sci.* **2010**, *34*, 210–216. [CrossRef]
19. Corcione, M. Empirical correlating equations for predicting the effective thermal conductivity and dynamic viscosity of nanofluids. *Energy Convers. Manag.* **2011**, *52*, 789–793. [CrossRef]
20. Einstein, A. *Investigations on the Theory of the Brownian Movement*; Fürth, R., Ed.; Courier Corporation: Chelmsford, MA, USA, 1956.
21. Gonçalves, I.; Souza, R.; Coutinho, G.; Miranda, J.; Moita, A.; Pereira, J.E.; Moreira, A.; Lima, R. Thermal Conductivity of Nanofluids: A Review on Prediction Models, Controversies and Challenges. *Appl. Sci.* **2021**, *11*, 2525. [CrossRef]

22. Kaplan, M.; Özdinç Çarpınlıoğlu, M. Proposed new equations for calculation of thermophysical properties of nanofluids. *Int. Adv. Res. Eng. J.* **2022**, *5*, 142–151. [CrossRef]
23. Zendehboudi, A.; Saidur, R. A reliable model to estimate the effective thermal conductivity of nanofluids. *Heat Mass Transf.* **2019**, *55*, 397–411. [CrossRef]
24. Sarkar, J.; Ghosh, P.; Adil, A. A review on hybrid nanofluids: Recent research, development and applications. *Renew. Sustain. Energy Rev.* **2015**, *43*, 164–177. [CrossRef]
25. Gupta, M.; Singh, V.; Kumar, S.; Kumar, S.; Dilbaghi, N.; Said, Z. Up to date review on the synthesis and thermophysical properties of hybrid nanofluids. *J. Clean. Prod.* **2018**, *190*, 169–192. [CrossRef]
26. Sundar, L.S.; Sharma, K.V.; Singh, M.K.; Sousa, A.C.M. Hybrid nanofluids preparation, thermal properties, heat transfer and friction factor—A review. *Renew. Sustain. Energy Rev.* **2017**, *68*, 185–198. [CrossRef]
27. Qi, C.; Wan, Y.L.; Wang, G.Q.; Han, D.T. Study on stabilities, thermophysical properties and natural convective heat transfer characteristics of TiO_2-water nanofluids. *Indian J. Phys.* **2018**, *92*, 461–478. [CrossRef]
28. Das, P.K.; Mallik, A.K.; Ganguly, R.; Santra, A.K. Synthesis and characterization of TiO_2–water nanofluids with different surfactants. *Int. Commun. Heat Mass Transf.* **2016**, *75*, 341–348. [CrossRef]
29. Alkasmoul, F.S.; Al-Asadi, M.T.; Myers, T.G.; Thompson, H.M.; Wilson, M.C.T. A practical evaluation of the performance of Al_2O_3-water, TiO_2-water and CuO-water nanofluids for convective cooling. *Int. J. Heat Mass Transf.* **2018**, *126*, 639–651. [CrossRef]
30. Garud, K.S.; Lee, M.-Y. Numerical Investigations on Heat Transfer Characteristics of Single Particle and Hybrid Nanofluids in Uniformly Heated Tube. *Symmetry* **2021**, *13*, 876. [CrossRef]
31. Javadi, H.; Urchueguia, J.F.; Mousavi Ajarostaghi, S.S.; Badenes, B. Impact of Employing Hybrid Nanofluids as Heat Carrier Fluid on the Thermal Performance of a Borehole Heat Exchanger. *Energies* **2021**, *14*, 2892. [CrossRef]
32. Khaleduzzaman, S.S.; Saidur, R.; Mahbubul, I.M.; Ward, T.A.; Sohel, M.R.; Shahrul, I.M.; Selvaraj, J.; Rahman, M.M. Energy, Exergy, and Friction Factor Analysis of Nanofluid as a Coolant for Electronics. *Ind. Eng. Chem. Res.* **2014**, *53*, 10512–10518. [CrossRef]
33. Khetib, Y.; Abo-Dief, H.M.; Alanazi, A.K.; Said, Z.; Memon, S.; Bhattacharyya, S.; Sharifpur, M. The Influence of Forced Convective Heat Transfer on Hybrid Nanofluid Flow in a Heat Exchanger with Elliptical Corrugated Tubes: Numerical Analyses and Optimization. *Appl. Sci.* **2022**, *12*, 2780. [CrossRef]
34. Senthilkumar, A.P.; Karthikeyan, P.; Janaki, S.; Reddy, E.P.; Rahman, Z.W.; Raajasimman, G. Effectiveness study on Al_2O_3-TiO_2 nanofluid heat exchanger. *Int. J. Eng. Robot Technol.* **2016**, *3*, 73–81.
35. Hamid, K.A.; Azmi, W.H.; Nabil, M.F.; Mamat, R.; Sharma, K.V. Experimental investigation of thermal conductivity and dynamic viscosity on nanoparticle mixture ratios of TiO_2-SiO_2 nanofluids. *Int. J. Heat Mass Transf.* **2018**, *116*, 1143–1152. [CrossRef]
36. Charab, A.A.; Movahedirad, S.; Norouzbeigi, R. Thermal conductivity of Al_2O_3 + TiO_2/water nanofluid: Model development and experimental validation. *Appl. Therm. Eng.* **2017**, *119*, 42–51. [CrossRef]
37. Garud, K.S.; Hwang, S.-G.; Lim, T.-K.; Kim, N.; Lee, M.-Y. First and Second Law Thermodynamic Analyses of Hybrid Nanofluid with Different Particle Shapes in a Microplate Heat Exchanger. *Symmetry* **2021**, *13*, 1466. [CrossRef]
38. Elias, M.M.; Shahrul, I.M.; Mahbubul, I.M.; Saidur, R.; Rahim, N.A. Effect of different nanoparticle shapes on shell and tube heat exchanger using different baffle angles and operated with nanofluid. *Int. J. Heat Mass Transf.* **2014**, *70*, 289–297. [CrossRef]
39. Chougule, S.S.; Sahu, S.K. Model of heat conduction in hybrid nanofluid. In Proceedings of the 2013 IEEE International Conference ON Emerging Trends in Computing, Communication and Nanotechnology (ICECCN), Tirunelveli, India, 25–26 March 2013; pp. 337–341.
40. Esfahani, N.N.; Toghraie, D.; Afrand, M. A new correlation for predicting the thermal conductivity of ZnO–Ag (50%–50%)/water hybrid nanofluid: An experimental study. *Powder Technol.* **2018**, *323*, 367–373. [CrossRef]
41. Hemmat Esfe, M.; Abbasian Arani, A.A.; Rezaie, M.; Yan, W.-M.; Karimipour, A. Experimental determination of thermal conductivity and dynamic viscosity of Ag–MgO/water hybrid nanofluid. *Int. Commun. Heat Mass Transf.* **2015**, *66*, 189–195. [CrossRef]
42. Hemmat Esfe, M.; Saedodin, S.; Biglari, M.; Rostamian, H. Experimental investigation of thermal conductivity of CNTs-Al2O3/water: A statistical approach. *Int. Commun. Heat Mass Transf.* **2015**, *69*, 29–33. [CrossRef]
43. Takabi, B.; Salehi, S. Augmentation of the Heat Transfer Performance of a Sinusoidal Corrugated Enclosure by Employing Hybrid Nanofluid. *Adv. Mech. Eng.* **2014**, *6*, 147059. [CrossRef]
44. Zadkhast, M.; Toghraie, D.; Karimipour, A. Developing a new correlation to estimate the thermal conductivity of MWCNT-CuO/water hybrid nanofluid via an experimental investigation. *J. Therm. Anal. Calorim.* **2017**, *129*, 859–867. [CrossRef]
45. Afrand, M.; Nazari Najafabadi, K.; Akbari, M. Effects of temperature and solid volume fraction on viscosity of SiO_2-MWCNTs/SAE40 hybrid nanofluid as a coolant and lubricant in heat engines. *Appl. Therm. Eng.* **2016**, *102*, 45–54. [CrossRef]
46. Asadi, A.; Asadi, M.; Rezaei, M.; Siahmargoi, M.; Asadi, F. The effect of temperature and solid concentration on dynamic viscosity of MWCNT/MgO (20–80)–SAE50 hybrid nano-lubricant and proposing a new correlation: An experimental study. *Int. Commun. Heat Mass Transf.* **2016**, *78*, 48–53. [CrossRef]
47. Dardan, E.; Afrand, M.; Meghdadi Isfahani, A.H. Effect of suspending hybrid nano-additives on rheological behavior of engine oil and pumping power. *Appl. Therm. Eng.* **2016**, *109*, 524–534. [CrossRef]
48. Soltani, O.; Akbari, M. Effects of temperature and particles concentration on the dynamic viscosity of MgO-MWCNT/ethylene glycol hybrid nanofluid: Experimental study. *Phys. E Low-Dimens. Syst. Nanostruct.* **2016**, *84*, 564–570. [CrossRef]

49. Bhattad, A.; Sarkar, J.; Ghosh, P. Energetic and Exergetic Performances of Plate Heat Exchanger Using Brine-Based Hybrid Nanofluid for Milk Chilling Application. *Heat Transf. Eng.* **2020**, *41*, 522–535. [CrossRef]
50. Bhattad, A.; Sarkar, J.; Ghosh, P. Heat transfer characteristics of plate heat exchanger using hybrid nanofluids: Effect of nanoparticle mixture ratio. *Heat Mass Transf.* **2020**, *56*, 2457–2472. [CrossRef]
51. Maddah, H.; Aghayari, R.; Mirzaee, M.; Ahmadi, M.H.; Sadeghzadeh, M.; Chamkha, A.J. Factorial experimental design for the thermal performance of a double pipe heat exchanger using Al_2O_3-TiO_2 hybrid nanofluid. *Int. Commun. Heat Mass Transf.* **2018**, *97*, 92–102. [CrossRef]
52. Hamid, K.A.; Azmi, W.H.; Nabil, M.F.; Mamat, R. Experimental investigation of nanoparticle mixture ratios on TiO_2–SiO_2 nanofluids heat transfer performance under turbulent flow. *Int. J. Heat Mass Transf.* **2018**, *118*, 617–627. [CrossRef]
53. Herwig, H. What Exactly is the Nusselt Number in Convective Heat Transfer Problems and are There Alternatives? *Entropy* **2016**, *18*, 198. [CrossRef]
54. Kakaç, S.; Liu, H.; Pramuanjaroenkij, A. *Heat Exchangers: Selection, Rating, and Thermal Design*, 4th ed.; CRC Press: Boca Raton, FL, USA, 2020.
55. Tiwari, A.K.; Ghosh, P.; Sarkar, J. Investigation of thermal conductivity and viscosity of Al_2O_3-water nanofluids. *J. Environ. Res. Dev.* **2012**, *7*, 768–777.
56. Bhattad, A.; Sarkar, J.; Ghosh, P. Experimentation on effect of particle ratio on hydrothermal performance of plate heat exchanger using hybrid nanofluid. *Appl. Therm. Eng.* **2019**, *162*, 114309. [CrossRef]
57. Eid, M.R.; Nafe, M.A. Thermal conductivity variation and heat generation effects on magneto-hybrid nanofluid flow in a porous medium with slip condition. *Waves Random Complex Media* **2022**, *32*, 1103–1127. [CrossRef]